An Approach to Predict the Slow Cook-off Response of Confined and Vented Full-Scale Munitions Based on Small Scale Tests

N. Albert Moussa and Vijay V. Devarakonda, BlazeTech Corp., Woburn MA; Michael J. Kaneshige, Sandia National Laboratories, Albuquerque, NM; and Lori Nock, NSWC IHEODTD N00174

NDIA Insensitive Munitions and Energetic Materials Technology Symposium, April, 2018, Portland, OR

Abstract

We have developed an approach to predict the cook-off response of confined and vented full-scale munitions based on small scale testing and analysis. This approach has 4 steps: (1) Measure the thermal degradation rates of confined and vented explosive versus temperature through small scale tests (~2 g of explosive per test), (2) Measure the burn rates of pristine, heated and thermally degraded explosive in a strand burner (~3 g of explosive/test), (3) Capture the above processes in a fast running cook-off model that includes algorithms for thermal degradation kinetics versus temperature and venting (from step 1), and burn rate versus temperature, pressure, extent of thermal degradation and venting (step 2), and (4) Validate the model by comparing its predictions with cook-off test data.

A summary of key findings from the implementation of the above approach to PBXN-111 follows:

- The rate of thermal degradation depends on temperature and confinement. For example, the mass loss of confined PBXN-111 due to thermal degradation increases from 0.74% in 32.6 hours at 151.8°C to 13.2% in 5.8 hours at 175.7°C. The initial thermal degradation rates of confined and vented PBXN-111 are almost identical, but at later times the rate of reaction is higher in confined systems.
- Up to 2000 psig, the burn rate of PBXN-111 is almost independent of temperature, pressure and time but it increases marginally (up to 7.5 times) with the extent of thermal degradation. Above 2000 psig, the burn rate increases significantly with the extent of thermal degradation and pressure. We observed up to ~3 orders of magnitude increase in burn rate due to a combination of thermal degradation and pressure.
- The wall temperature required for ignition increases with heating rate.

BlazeTech's thermal degradation, burn rate and cook-off tests with PBXN-111 are presented along with the data analysis and model development. We find that tracking the pressure evolution (while ignored by others) is critical to proper modelling of slow cook-off.

Introduction

Historical data (USS Oriskany 1966, USS Forestall 1967, USS Enterprise 1969 and USS Nimitz 1981) suggest that accidents involving energetic materials and munitions can lead to large scale damage during regular military operations. This has prompted the DOD and DOE to develop Insensitive Munitions (IM) that are safe under normal conditions but can be activated on-demand under a narrow range of conditions. However, the explosive formulations being evaluated as IMs can cook-off when exposed to heat. Cook-off response is commonly studied using full scale tests that are time and resource intensive. In addition to developing safer chemistries, the research community is examining safety methods such as latent venting to protect against various types of hazards. We developed an innovative approach to evaluate the safety of new formulations to cook-off and develop vent design parameters. Our approach consists of a coordinated set of small scale tests and modeling covering thermal degradation, ignition, combustion and venting. It was implemented on the slow cookoff of PBXN-111 through a Phase II SBIR project funded by the US Navy and it can be applied to other munition formulations. PBXN-111 consists of 43% ammonium perchlorate, 25% aluminum, 20% RDX, and 12% HTPB/IDP binder system. Our models can also be used to design vents to lower the cook-off violence and are equally valid to fast cook-off. Our approach consists of four steps described in this paper.

Thermal Degradation of PBXN-111

The first step is to develop thermal degradation kinetics through controlled tests and analysis. PBXN-111 undergoes exothermic thermal degradation reactions at increasing rates when heated causing it to self-heat and eventually ignite. Focusing on these pre-ignition reactions, we developed a small-scale test where the thermal degradation rate can be measured accurately through controlled tests on ~2 g of explosive per test. The explosive is loaded into a steel casing and placed in a larger aluminum oven shown in Figure 1 (mid and right photographs). It is heated to a target temperature between 150° and 180°C where it is held for several hours either under completely confined or vented conditions and the heat was turned off before the material can ignite. The small size ensures that the entire test setup heats up uniformly with no temperature gradients during the test. We used 3 thermocouples (TC1, TC2 and Control) to measure the steel casing temperature and one to measure the explosive temperatures during the tests. The confined test setup is also equipped with a pressure sensor to measure the pressure-time history due to thermal degradation. In each test, we carefully measured the dimensions and masses of about 6 cylindrical PBXN-111 pellets which were then loaded into the test fixture. We measured the temperature-time histories during the test, the overall mass loss after the test and for the confined tests the pressure-time histories.

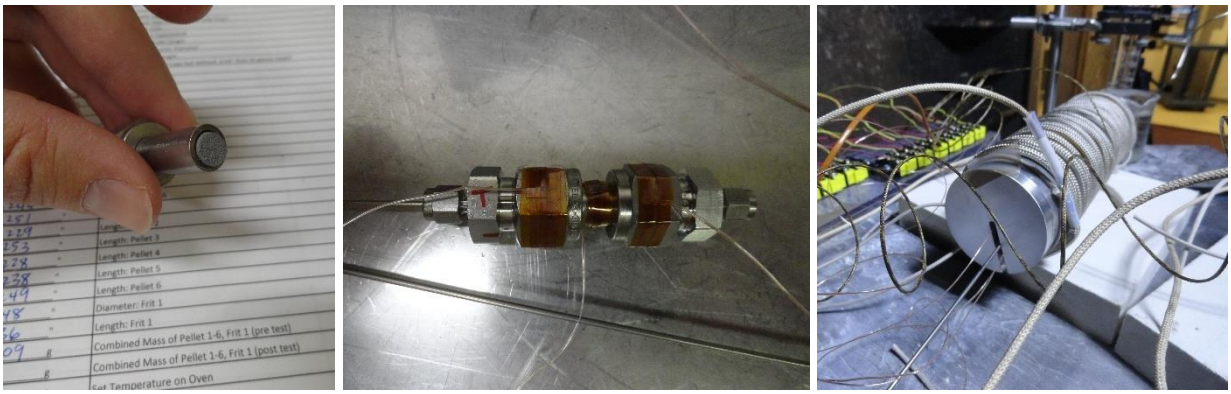

Figure 1: Photographs of apparatus assembly for the thermal degradation tests on confined and vented PBXN-111.

We performed 8 tests each with confined and vented PBXN-111 varying the temperature and exposure time. Sample data from one of these tests (Con-114) in which confined PBXN-111 was heated to 160.3°C for 17.2 hours are shown in Figure 2. At the start of each test, we heated the oven to a slightly higher temperature than the target value to ensure that the steel casing and the explosive reach the target temperature in only a few minutes as shown in Figure 2 (a). RDX-based explosives like PBXN-111 degrade slowly below 130°C, so we focused on the duration for which the test apparatus remains hotter than 130°C. The close agreement between the temperature-time histories recorded by the 4 thermocouples shows that the temperature was uniform throughout the test setup. The explosive heated up more than the casing at later times suggesting the occurrence of exothermic reactions. We turned the oven off at ~1000 minutes and allowed the system to cool down to ambient temperature. The pressure increased slowly with time initially, before accelerating later due to rapid gas and heat release from thermal degradation reactions reaching a maximum of 723 psig when the heat was turned off as shown in Figure 2 (b). The pressure then decreased gradually as the system cooled down. Focusing on the period when the explosive remained hotter than 130°C, we determined the time-averaged temperature. The test conditions as well as the measured mass losses from the confined tests are summarized in Table 1. These results show that at a given temperature, the mass loss due to thermal degradation (i.e., the extent of reaction) increases with time. The mass loss rate is slow initially, but increases with time. The mass loss rate increases with temperature from 151.8°C (Con-108) to 175.7°C (Con-116). We performed 8 such tests on vented PBXN-111 and the results from

these tests are presented in Table 2. The initial mass loss rates are comparable in confined and vented PBXN-111, but later the confined PBXN-111 degraded faster than the vented material.

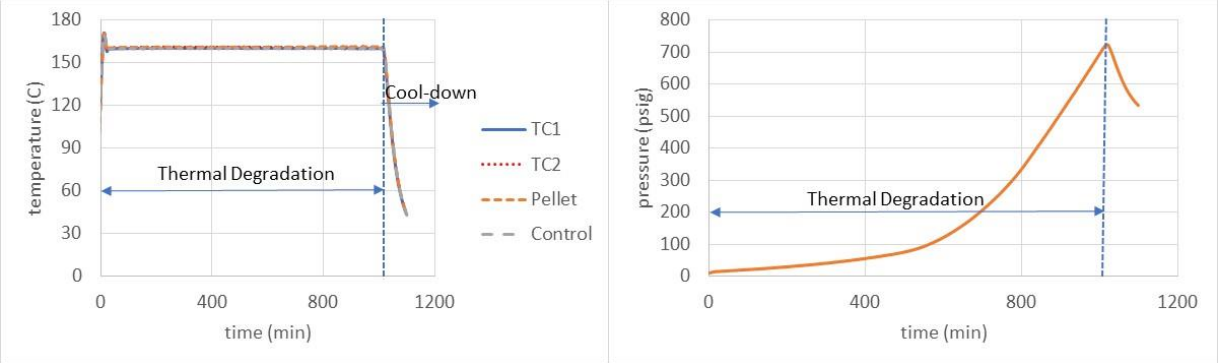

Figure 2: Temperature and pressure versus time data collected from thermal degradation test Con-114 in which confined PBXN-111 heated to 160.3 C for 17.2 hours.

Table 1: Summary of test conditions and key results from thermal degradation tests on confined PBXN-111.

Test No. Con-	*t* (min)	Temperature (°C)			P (psig)			*Explosive Mass (g)*		Mass Loss, %
		T_{mean}	T_{peak}	T_f	P_i	P_{peak}	P_f	Initial	Final	
108	1955	151.8	156.5	31.2	2.4	80.7	48.6	2.109	2.078	0.74
102	246	160.1	163.4	160.1	3.2	30.5	NM	2.120	2.112	0.41
104	500	160.1	165	21.6	4.2	65.2	32.2	2.136	2.126	0.47
114	1031	160.3	170.6	43.8	4.9	723	534	2.065	1.960	5.05
106	266	168.9	174	35.8	2.7	130	81	2.162	2.134	1.27
110	506	169.6	174.9	33	3.1	1220	953	2.164	1.947	10.0
112	267	174.3	184.7	54.8	10.4	888	697	2.017	1.890	6.3
116	349	175.7	182.2	25.6	2.5	1104	NM	2.129	1.847	13.2

Table 2: Summary of test conditions and key results from thermal degradation tests on vented PBXN-111.

Test No.	Duration (min)	Temperature (°C)	Mass Loss (%)
Con109	1955	147.4	0.86
Con103	246.3	158.4	0.52
Con105	502.2	159.9	0.68
Con115	1030	160.1	2.93
Con107	264.4	167.5	1.4
Con111	505.6	169.3	4.7
Con113	266	173.2	6.8
Con117	350.2	174.2	11.9

We converted the pressure-time histories from each confined test into residual explosive mass versus time data, fitted a two-step first order reaction model through these data, and determined the rate constants for each step. The logarithmic rate constants from the two steps are plotted as functions of reciprocal temperature in the left of Figure 3 and determined the Arrhenius rate parameters from the slope and the y-intercept. The rate constant increased with temperature, but we obtained close agreement in the rate constants of various tests conducted at a given temperature. For vented PBXN-111, we fitted a global one-step reaction model through the overall mass loss versus time data and these rate constants are plotted versus reciprocal temperature in the right of Figure 3. The confined and vented PBXN-111 reacted at similar rates at the beginning,

but the pressure buildup with time increased the reaction rate of the former. The reaction rates were very slow below 150°C, but they increased significantly at higher temperatures: the rate constants (for both confined and vented PBXN-111) increased by more than 1 order of magnitude with temperature from 151.8°C to 175.7°C.

We have presented an innovative approach based on small scale tests and analysis to develop the thermal degradation reaction rate kinetics of confined and vented explosives. The rate kinetics models for PBXN-111 are now ready for integration into the cook-off model.

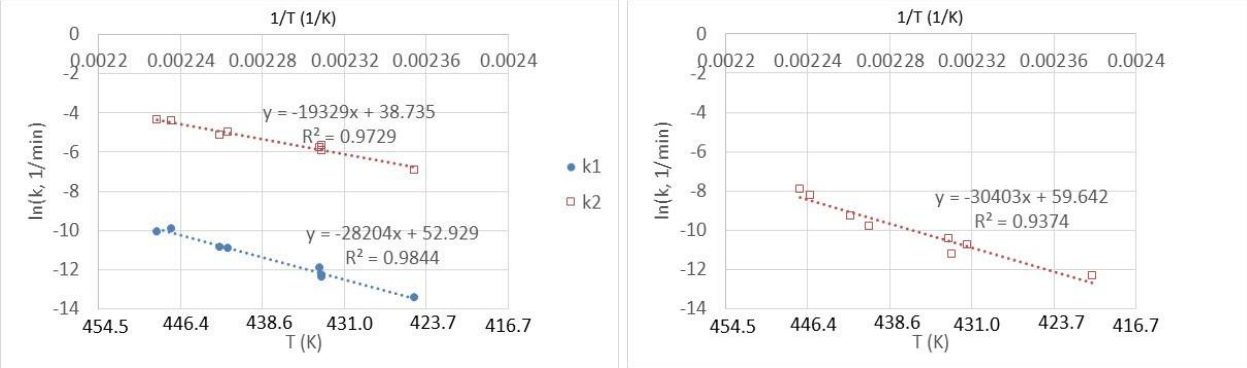

Figure 3: The rate constants for thermal degradation of confined (left) and vented (right) PBXN-111.

Combustion of PBXN-111

Upon ignition, the combustion front propagates through the explosive raising the pressure rapidly. Focusing on these fast processes, we performed burn rate measurements on pristine, heated (but undegraded), and heated and degraded PBXN-111 as functions of pressure in a strand burner. We made three key changes to the traditional strand burner measurements and the data analysis: (i) we reduced the empty space inside the burner chamber to improve confinement and facilitate secondary reactions of PBXN-111 thermal degradation products, (ii) we inserted thermocouples and break wires inside the explosive strand to track the strand temperature as well as the burn front location versus time during the burn test, and (iii) we used both the pressure-time histories and the thermocouple/break wire data to generate *x-t* diagrams for the burn front. We attached the individual explosive pellets, ignitor, thermocouples (yellow wires in the left of Figure 4) and the break wires (red wires) to the sample holder before installing the sample holder inside the strand burner. A schematic of the overall setup is shown in the right of Figure 4. In each test, we measured the pressures (3 sensors), temperatures (2 locations along the strand) and signals from 5 break wires versus time, and the time of ignition (from ignitor data).

We conducted 10 burn tests varying the temperature, extent of degradation and initial pressure at ignition. Sample data from test HPSB-049 in which the strand was heated to 160°C for 17 hours prior to ignition are shown in Figure 5. It took ~3 hours to heat the strand burner and the explosive pellets from room temperature to ~160°C due to the large thermal mass of the strand burner (equipped with thick walls to withstand pressures generated during the burn test). The system remained close to 160°C during the thermal degradation phase, with the top of the strand being slightly warmer than the bottom. Once the strand was ignited, the burn test lasted only about 2 s. The strand burner was filled with an inert gas to generate an initial pressure of ~1000 psig before the onset of heating. The 3 pressure transducers responded differently to the temperature rise and exhibited some variability as shown in the figure. The pressure increased slightly during the 17-hour thermal degradation due to the release of thermal degradation products and the temperature becoming more uniform in the strand burner. Upon ignition, the pressure increased rapidly as shown in Figure 5 (b).

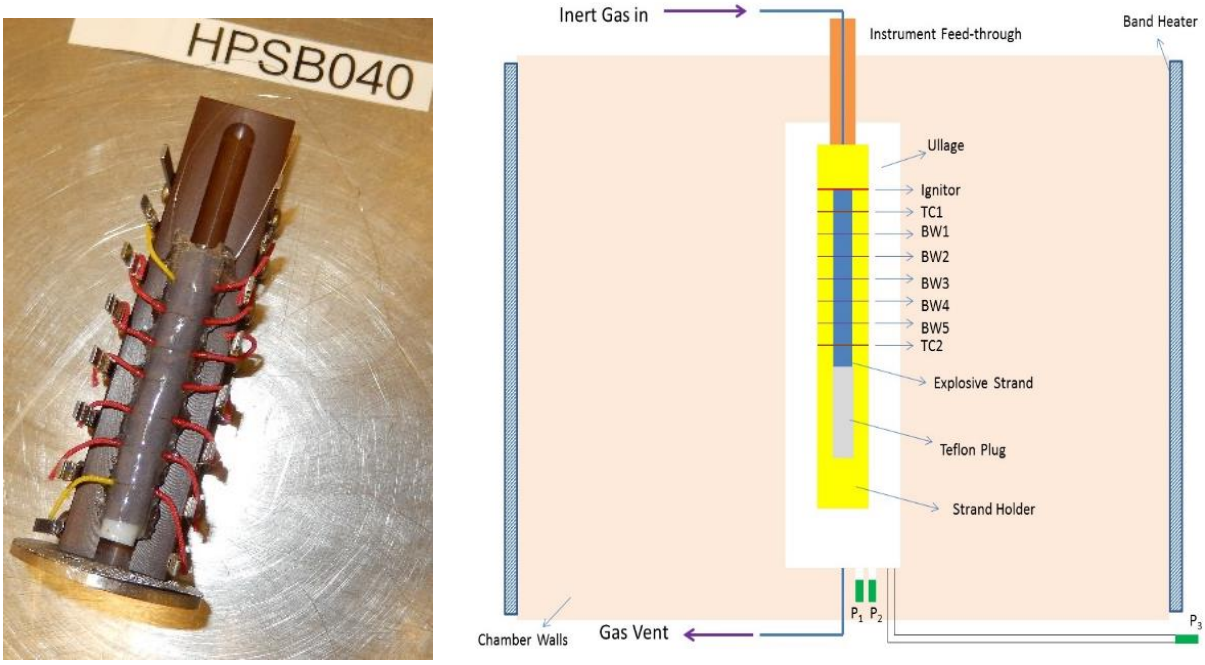

Figure 4: Installation of explosive pellets, ignitor, thermocouples, and break wires inside the sample holder; and the schematic of the strand burner apparatus.

The normalized signals from the ignitor located at the top of the strand, 2 thermocouples (TC1 located between the top 2 explosive pellets and TC2 between the bottom two), and the 5 breakwires, plotted in Figure 5 (c), show that the burn front moved from the top of the strand (ignitor location) to the bottom sequentially triggering each sensor along the way. The burn rate was slow initially and consumed the top pellet in 0.45 s, but accelerated later as it consumed the bottom pellet in only ~0.1 s. This acceleration is also evident from the narrowing of the gap between the triggering times of successive sensors as shown in Figure 5 (c). The pressure increased from ~1080 psig at ignition to ~2550 psig at the end of combustion as shown in Figure 5 (d). The rate of pressure rise increased during the test, also suggesting burn front acceleration. The small discontinuities in the pressure plots could be due to the small gaps between successive pellets introduced by the insertion of sensors. We interpreted the signals from the ignitor, thermocouples and the break wires in each test to track the burn front versus time. In a few tests, the break wires did not get triggered sequentially possibly due to electronic cross-talk and/or failure of the epoxy coating that caused the burn front to run down the sides of the explosive. We developed an alternate technique based on the pressure data to generate the *x-t* plots for the burn propagation. We fitted second order polynomials through these plots and determined the burn rates and accelerations from first and second time derivatives of these fits.

The test conditions such as the test id, strand temperature at ignition, time averaged strand temperature, duration for which the strand remains above 130°C, pressure at ignition and the peak pressure at the end of combustion are presented in the first 6 columns of Table 3. The extents of thermal degradation at ignition (ϕ calculated using our kinetics model) are presented in column 7. We fitted the power law model (below) through the burn rate versus pressure data obtained from each test and determined the burn rate parameters *A* and *n*. The burn rate increases significantly when the pressure exceeds ~2000 psig (13.8 MPa), so we generated separate fits for the data below and above 2000 psig. The fit parameters are presented in columns 8, 9, 11 and 12 of Table 3 for the following equation with *u* given in cm/s, *P* in MPa and ϕ in %:

$$u = A(\phi) \times P^{n(\phi)}$$

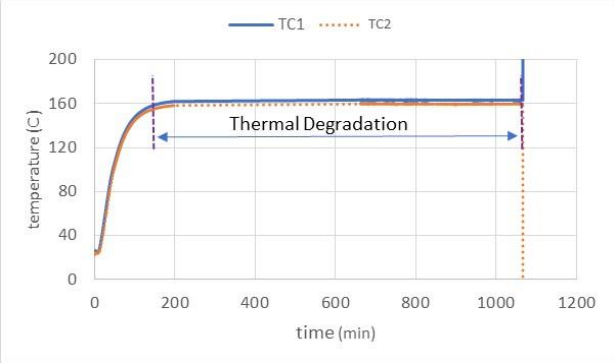

(a) Temperature-time history.

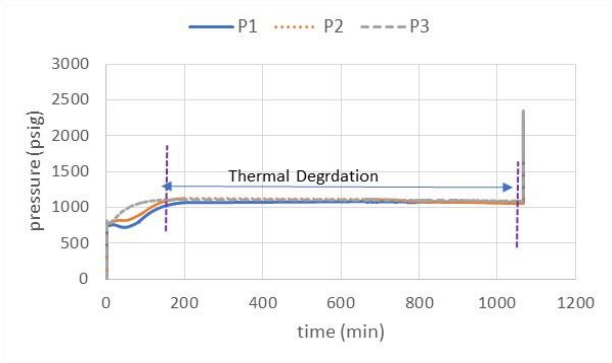

(b) Pressure-time histories.

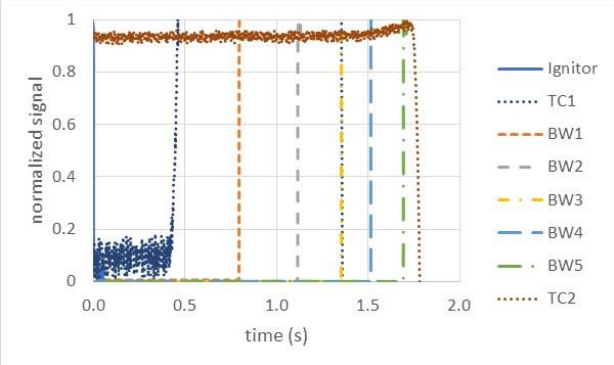

(c) Ignitor, thermocouples and break wires data.

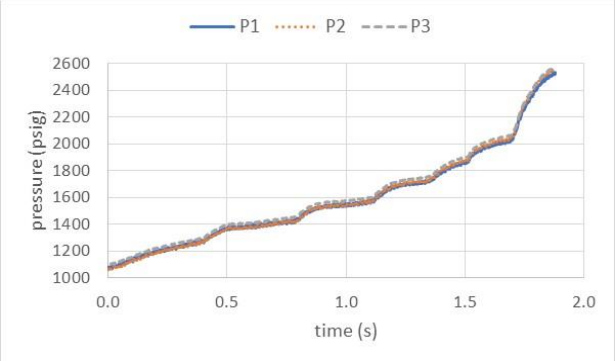

(d) Pressure-time histories after ignition.

Figure 5: Burn test HPSB049 in which PBXN-111 strand was thermally degraded for 17.2 hours at 160°C before ignition.

Pristine PBXN-111 at room temperature burned at a constant speed of 0.55 cm/s. Four tests with heated, but un-degraded explosive showed that the burn rate increased to 0.87 cm/s at 160°C and further to 0.93 cm/s at 175°C. These data suggest that the burn rate remains constant at 0.9 ±0.03 cm/s and is almost independent of temperature between 160° and 175°C. Pressure has almost no effect on burn rate of undegraded PBXN-111 below 2000 psig, and so the value of *n* remains at 0 as shown in column 9. Above 2000 psig, the burn rate of undegraded PBXN-111 is weakly dependent on pressure (i.e., *n* ~0), while that of degraded material becomes increasingly sensitive to pressure (i.e., *n* increases with the extent of degradation). Since the burn rate increases with pressure, the combustion front accelerates with time in degraded PBXN-111, the magnitude of acceleration increasing with the extent of thermal degradation as shown in column 10 of the table. We observed increases of ~3 orders of magnitude in burn rate due to thermal degradation and pressure. We generated fits for the burn rate parameters *A* and *n* as functions of the extent of thermal degradation ϕ (which can be improved with additional data). These fits are used in our combustion model.

Models for Ignition, Combustion and Venting

We developed two separate fast-running engineering models to capture cook-off: ignition model to track the various processes that occur until ignition, and the combustion model to track the burn propagation through the explosive after ignition. The ignition model tracks the heat conduction from the casing walls to the explosive as well as within the explosive; thermal expansion of the explosive that in turn compresses the gases; thermal degradation and resulting porosity generation; changes in the rate of thermal degradation reactions due to venting; changes in the pressure due to heating, heat and gas generation from thermal degradation reactions, and gas loss due to venting; and ignition of the explosive when the local temperature significantly exceeds the externally imposed wall temperature. The model inputs include: dimensions of the explosive, ullage and the casing, heating profile (including the soak), and the vent parameters (pressure

needed for vent activation and the vent diameter). The model outputs the pressure, temperature and extent of reaction profiles throughout the explosive versus time until ignition, occurrence of ignition, and the time and location of ignition.

Table 3: Summary of conditions and key results from burn rate tests with pristine, heated and degraded PBXN-111.

	Measurements					Analysis					
Test	**$T^{\#}$ (°C)**		**$t_{soak}^{\$}$**	**P (psig)**		**ϕ**	**Initial**		**Later**		
HPSB	**$T_{ign}^{\&}$**	**T_{ave}***	**(min)**	**P_{ign}**	**P_{final}**	**(%)**	**A (cm/s)**	**n**	**a (cm/s^2)**	**A (cm/s)**	**n**
040**	22	22	0	0		0.00	0.23	0	0	NA	NA
041**	22	22	0	990	1880	0.00	0.55	0	0	NA	NA
046	161.8	156	7.1	1020	2110	0.00	0.87	0	0	NA	NA
049**	**163**	**162.5**	**950**	**1080**	**2550**	**4.50**	**1.81**	**0**	**13.3**	**0.22**	**1.23**
048	170	160.7	13.3	1050	2210	0.01	0.87	0	0	NA	NA
051	170.1	160.9	11.4	2630	5080	0.01	1.59	0	0	NA	NA
047	**173.8**	**171.7**	**485**	**1450**	**3130**	**18.2**	**3.5**	**0**	**79.4**	**0.22**	**1.57**
050**	**171.1**	**169.3**	**480**	**2090**	**4240**	**6.35**	**1.96**	**0**	**42.7**	**0.22**	**1.23**
043	175	172.7	3.5	1190	2650	0.03	0.93	0	2.34	0.22	0.96
044	**177.3**	**175.8**	**239**	**1590**	**4510**	**7.38**	**6.5**	**0**	**27,784**	**0.22**	**2.34**

* time averaged temperature near the strand top over the duration of thermal degradation reactions
\# temperatures near the strand top between pellets 1 & 2 & at the time of ignition
\$ duration for which the strand remains above 150°C ** leaks occurred during the test

We performed several parametric calculations with this model, and we present the results from one calculation here for illustration. We considered the Navy sub-scale test 1 [Refs. 1 and 2]) with 6690 g of PBXN-111 with a diameter of 14.74 cm and a length of 21.9 cm and heated in 3 steps: (i) rapid heating from $T_{ambient}$ to 65.6°C, (ii) 8 hour soak, and (iii) slow heating at 0.052°C/min until ignition. We assumed a confined system with no vent here. In the test, the explosive material ignited about 1960 min after soak when the explosive wall reached 166.5±1°C. The model predicts the temperature and extent of thermal degradation reaction distributions throughout the explosive as well as the quasi-static pressure versus time until ignition. The model assumes that the explosive surface remains in thermal equilibrium with the casing. Initially, the casing is hotter than the explosive, so heat is transferred from the explosive surface to the center. When the explosive reaches ~150°C, it undergoes exothermic reactions causing the material to self-heat. The casing wall quenches the surface of the explosive, but the heat released in the inner core remains trapped locally in the explosive. This causes the inner regions of the explosive to heat up more than the surface at later times changing the direction of heat transfer. We assumed that ignition occurs when the hottest region in the explosive exceeds the externally imposed wall temperature by >10°C. Our model predicts that this occurs when the wall temperature reaches 169.6°C about 2018 minutes after the end of soak. The ullage pressure predicted by our model (Figure 6 (b)) shows a small initial increase due to the temperature rise of the gases in the ullage. The heat and the gas release from exothermic reactions when the explosive reaches ~150°C at 1640 minutes, raises the pressure at increasing rates as shown by the sharp rise in the pressure-time history in Figure 6 (b). The model predicts a pressure of 626 psig (4.3 MPa) at ignition.

Our combustion model uses the results from ignition calculations presented above as inputs and tracks the burn front propagation accounting for the heat and gas generation from combustion and the energy losses from the burned gases. The model inputs include: dimensions of the explosive, casing and the ullage; location of ignition; conditions at ignition such as the pressure and the mean extent of thermal degradation averaged across the explosive; and the vent parameters (onset pressure for venting and the vent diameter). The model outputs the time

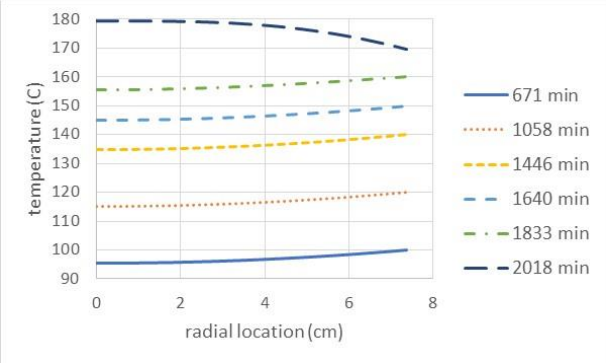

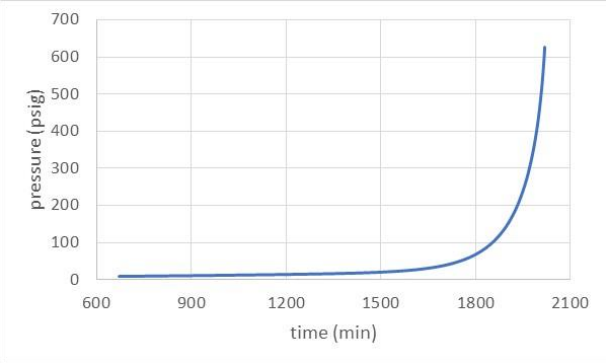

(a) Temperature profiles in the explosive until ignition. **(b) Quasi-static pressure versus time.**

Figure 6: Results from sample calculation with the ignition model for the conditions of the Navy sub-scale test 1 with 6690 g of PBXN-111 heated at 0.055°C/min until cookoff.

dependent pressure, burned gas temperature, masses of residual explosive and gases, and the dimensions of burned region. We present here the results from one calculation for the conditions of Navy sub-scale test 1 for illustration. We used the ignition results (ignition at center 2018 minutes after the end of soak when the wall reaches 169.6°C, pressure at ignition of 4.3 MPa, and the mean porosity of ~0.4%). We assumed that the container had no leaks and that it could withstand a pressure of 200 MPa. The pressure-time history predicted by the model is plotted in Figure 7 (a). Given that the extent of thermal degradation at ignition is small and the pressure is low, the initial burn rate is low and pressure-independent. Since ignition occurs at the center, the burn front propagates in the radially outward direction. The mass burning rate (defined as the product of the burn rate and the surface area of the burned region) increases steadily with time causing a similar increase in the heat release and gas generation rates, raising the pressure steadily with time to 13.8 MPa (or 2000 psig). The burn rate then becomes pressure dependent and increases with pressure. The increases in the burn rate as well as the surface area of the burned region then increase the mass consumption rate of the explosive. ~3 s after the ignition, the burn front reaches the external wall. Then the burn front propagates axially in both directions away from the center rapidly raising the pressure, burn rate and the mass consumption rate. The pressure soon reaches 200 MPa, the assumed failure pressure for the casing. The casing may fail at a lower pressure due to the potential weakening of the wall caused by heat. The masses of the residual explosive and the gases generated from combustion are plotted versus time in Figure 7 (b). The residual explosive mass decreases slowly with time as the burn front travels from the center to the explosive surface. It then decreases rapidly as the mass burning rate increases sharply with time. Similarly, the mass of gas generated increases slowly with time initially, before speeding up later. The results from the ignition and the combustion models appear reasonable and internally consistent and serve as model verification.

Model Validation

Limited PBXN-111 SCO test data are available in the literature to validate our ignition model but none for our combustion model. These involved ~6690 g (D = 2.9” and L = 8.6”) used in each of the Navy sub-scale tests [1,2] and ~57.6 g (diameter = 1” and length = 2.5”) in the Variable Confinement Cook-off Test (VCCT) [3]. In these tests, the explosive was heated at a constant rate until cook-off while monitoring the temperatures at select locations. We performed 9 small scale cook-off tests with ~2.1 g of PBXN-111 per test (D = 0.25” and L = 1.5”) to generate additional data at heating rates between 0.02° & 0.406°C/min and confinement levels. The input conditions as well as key results from all the cook-off tests (literature & BlazeTech) are summarized in Table 4. They cover ~1 order of magnitude variability each in size and heating rate for scaling analysis. Predictions from our ignition model for each set of test conditions are presented at the bottom of the table. Our predictions agree within ~3°C of the measurements

despite the large ranges in heating rates and sizes. These data show that at a given size, the wall temperature at ignition increases with heating rate. At a given heating rate, the wall temperature at ignition is (a) independent of radius up to ~0.5” and decreases as size increases above 0.5” (for slow heating rates that are commonly used in SCO tests), and (b) is independent of radius for fast heating rates. This serves as validation of our model. The utility of our model is that it yields additional information that is difficult to characterize such as the ignition location, extent of thermal degradation/porosity distribution until ignition, and the pressure at ignition.

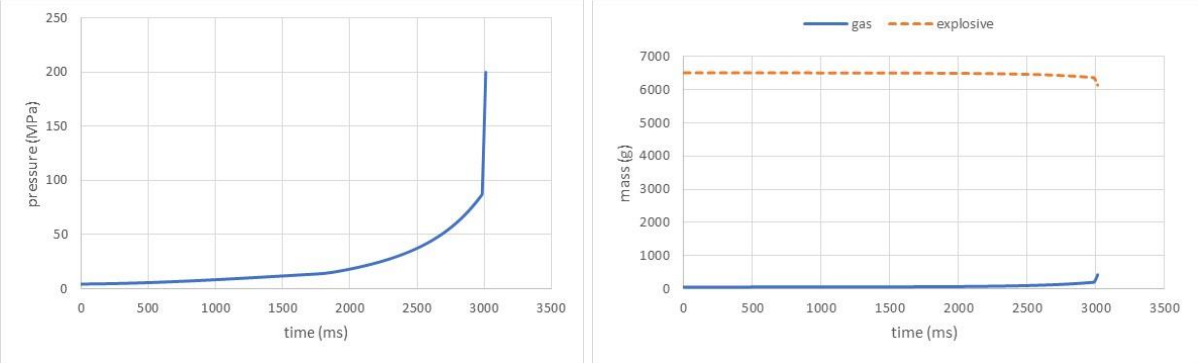

(a) Pressure-time history after ignition. **(b) Masses of residual explosive and gases.**

Figure 7: Results from sample calculation with the combustion model for the conditions from the Navy sub-scale test 1 with 6690 g of PBXN-111 heated at 0.055°C/min until cookoff.

Effect of Venting on Cook-Off

Latent venting can reduce the violence of cook-off as it affects both the thermal degradation reactions before ignition and the rate of combustion propagation after ignition of PBXN-111. A vent that opens early can discharge gaseous thermal degradation reaction intermediates and products from the munition into the atmosphere. Removal of these products eliminates their secondary reactions with the residual explosive as indicated by the fact that the thermal degradation rates are comparable in both the confined and vented PBXN-111 initially, but the confined material reacts faster than the vented one at later time. This suggests that when the munition is being heated slowly (under SCO conditions), a small vent that opens early should be adequate to reduce the pressure rise, because the rate of thermal degradation reaction is modest initially (provided the vent does not get clogged). In addition to reducing the extent of thermal degradation, venting reduces the pressure at ignition, which in turn affects the burn rate. If the vent gets activated at high pressures and opens after ignition, it can still help lower the violence of cook-off. This is because upon ignition, the burn rate of PBXN-111 depends mainly on pressure and the extent of thermal degradation. Burn rate remains low and constant for pressures below 2000 psig, but it increases significantly and becomes dependent on pressure and the extent of thermal degradation above 2000 psig. Therefore, a properly sized vent which ensures that the pressure remains below 2000 psig will reduce the violence of cook-off. Small-scale cookoff tests performed by BlazeTech/SNL have shown that completely confined PBXN-111 underwent cook-off leading to casing fragmentation. Exothermic reactions and mild self-heating occurred in a system with small leaks or a vent, but it did not cook-off. This suggests that venting is effective in reducing the violence of PBXN-111 cook-off. However, the vent needs to be designed and placed properly to ensure that it does not get clogged and remains effective.

Conclusions

We presented the implementation of our approach based on small scale tests and analysis to predict the slow cook-off violence of confined and vented PBXN-111. Our study showed that:

- The thermal degradation rate of PBXN-111 increases with temperature, time and confinement. Venting does not prevent self-heating, but it lowers the pressure at ignition.

- The burn rate of PBXN-111 is almost independent of temperature (if the material does not degrade during heating) and pressure below 2000 psig. Above 2000 psig, the burn rate becomes pressure-dependent in thermally degraded PBXN-111. Burn rate can increase by orders of magnitude due to pressure and thermal degradation.
- PBXN-111 cook-off can be captured using two models: (i) the ignition model predicts the temperature and extent of thermal degradation profiles and the pressure until ignition. Model predictions of ignition temperatures agree well with test data covering ~1 order of magnitude variability each in heating rates and size: serves as model validation. For slow heating rates (i.e., SCO conditions), the ignition temperature increases with heating rate (for a given size) and is independent of size below ~0.5", but it decreases with size above 0.5". For fast heating rates (FCO conditions), the ignition temperature is almost independent of size. The location of ignition shifts from the center towards the walls as the heating rate is increased. (ii) The combustion model predicts the burn front propagation, pressure, burned gas temperature, and residual explosive mass versus time.

The model presented here can be used to characterize the cook-off hazard, design vents to reduce the cook-off violence, and design future tests.

Table 4: Summary of test conditions and key results from the cook-off tests

Parameter	**BlazeTech SCO Tests (CCO-)**			**VCCT [3]**	**Sub-Scale [1,2]**	
Test id-	**100a, 100b, 101a**	**103a, 103b, 104b**	**102a, 102b**		**Test 1**	**Test 2**
Test Conditions						
$T_{ambient}$ (°C)	22	22	22	20*	20*	20*
Initial d*T*/d*t* (°C/min)	1.7	1.7	1.7	10*	10*	10*
T_{soak} (°C)	130	130	130	75	65.6	65.6
t_{soak} (min)	30	30	30	240	480	480
Final d*T*/d*t* (°C/min)	0.406	0.1	0.05	0.055	0.0515	0.479
Explosive Mass (g)	2.09	2.09	2.09	57.6	6690	6690
Ullage Volume (%)	45	45	45	10*	10*	10*
Explosive Radius (cm)	0.309	0.309	0.309	1.27	7.37	7.37
Explosive Length (cm)	3.8	3.8	3.8	6.35	21.9	21.9
Test Measurements						
T_{wall} at Ignition (°C)	195– 197.2	185.5–188	178.9–179.2	177 – 183	166.5	197.7
$t_{ignition}$ after soak (min)	160– 166	548– 589	976	1854- 1963	1960	276
Model Predictions						
T_{wall} at Ignition (°C)	197.1	187.1	181.7	176.0	169.6	194.8
$t_{ignition}$ after soak (min)	165	573	1029	1837	2018	270
Ignition Location	center	center	center	center	center	6.64 cm from center

References

1. Beckett, K.M., Oetjen, M., Gibson, K., Nock, L., and K. Clark, "Effect of heating rate on munition thermal profile, hotspot location and reaction violence",
2. Beckett, K.M., Oetjen, M., and K.D. Gibson, "The effects of heating rate and reaction location on violence in monolithic energetic configurations",
3. Nock. L.A., Lawrence, G.W., Sherlock, M.H., Gibson, K.D. and D.N. Sorensen, "Effect of binder systems on underwater explosive slow cook-off violence and interactions with warhead venting".

All 3 papers were presented at the 39th PEDCS, JANNAF, Salt Lake City, Utah, 12/7-10/2015.